# Intermittency Model for Coupled CFD-Stability Transition Analysis in Hypersonic Flows

Ethan A. Vogel* and Meelan Choudhari†
*NASA Langley Research Center, Hampton, VA, 23681*

**Accurate prediction of aerothermodynamic loads on hypersonic vehicles requires precise modeling of surface quantities across the boundary layer transition zone. The peak heating loads and total heat transfer are determined by parameters such as the transition zone length and the magnitude of potential overshoots in heat flux and skin friction beyond their respective values in fully turbulent flows. While previous studies on CFD integrated transition modeling using linear stability correlations have shown promise in modeling these features, they did not develop an intermittency model for hypersonic flows. This paper presents a data-driven approach to develop a model of this type by correlating experimental transition data with the relevant flow parameters. The resulting model demonstrates significant improvements over previous low-speed models in terms of predicting heat transfer distributions during the transition process associated with first and second mode instabilities in axisymmetric high-speed flows. Separate correlations for flight and ground test conditions are developed, and the potential to combine these correlations is discussed.**

## Nomenclature

| | | |
|---|---|---|
| $C_h$ | = | Stanton number |
| $C_{ov}$ | = | Intermittency overshoot parameter (nondimensional) |
| M | = | Mach number |
| $Re'$ | = | Reynolds number (nondimensional) |
| $Re_\infty$ | = | Freestream unit Reynolds number [1/m] |
| $\Delta Re$ | = | Nondimensional Intermittency width |
| $T$ | = | Temperature [K] |
| $Tu$ | = | Turbulence intensity [%] |
| $x$ | = | Streamwise position [mm] |
| $\alpha$ | = | Correlation plotting parameters (nondimensional) |
| $\Gamma$ | = | Observed (experimental) intermittency |
| $\gamma$ | = | Imposed (computational) intermittency |
| $\eta$ | = | Intermittency function exponent |
| $\lambda$ | = | Nondimensional pressure gradient |
| $\zeta$ | = | Nondimensionalized transition coordinate |
| *subscripts* | | |
| 1 | = | corresponding to transition upstream of overshoot peak |
| 2 | = | corresponding to transition downstream of overshoot peak |
| $\infty$ | = | Freestream value |
| $f$ | = | For use with flight test correlation |
| $onset$ | = | Value at onset of transition |
| $ov$ | = | Value at peak transition overshoot position |
| $t$ | = | For use with ground test facility correlation |
| $tot$ | = | Stagnation reference value |
| $turb$ | = | Value at the end of transition |
| $w$ | = | Value at the wall |

*Aerospace Technologist, Computational AeroSciences Branch, ethan.a.vogel@nasa.gov, AIAA Member
†Aerospace Technologist, Computational AeroSciences Branch, m.m.choudhari@nasa.gov, AIAA Fellow

# I. Introduction

Laminar-turbulent transition prediction is critical for the advancement of high-speed systems design [1]. Among the most important engineering impacts of transition are the change in total heat load relative to purely laminar or purely turbulent flows as well as the local peak in surface heat flux that is often seen near the end of the transition region. The later overshoot dictates the peak local surface heating and substantially contributes to the integrated heat load over the system. In recent literature, efforts related to Reynolds-averaged Navier-Stokes (RANS)-integrated transition prediction has focused on the correct identification of the transition location. While this is a necessary aspect of transition prediction, adequate characterization of the overall heating experienced by a body also requires that the heating in the neighborhood of the transition point be adequately characterized. Features such as the transition region's extent and the presence and degree of transition overshoot (where the local heat transfer in the transition zone exceeds that of the expected fully turbulent case) are relevant to the total heat load experienced by the body. In order for CFD analysis that includes transition prediction to provide highly-accurate predictions of relevant engineering quantities, not only must the onset of transition be placed appropriately on the body, but the heating characteristics of the transition zone itself must be predicted as well.

In the context of RANS-based modeling, transition is often examined in terms of intermittency, denoted here as $\Gamma$ when referencing physical or experimental contexts, and $\gamma$ when discussing CFD. When referring to experimental data, intermittency describes the fraction of time that the flow at a given point in space remains turbulent [2]. Intermittency is 0 in fully laminar flow and 1 in fully turbulent flow, and the transition zone is defined as the region where $0 < \Gamma < 1$. In time-averaged computations such as RANS, intermittency is a parameter that modifies the activation of turbulence modeling equations or multiplies turbulence modeling parameters to replicate the mean flow characteristics associated with transition. In RANS computations, intermittency values greater than one may be utilized as a means of replicating transitional overshoot of turbulent heating. Overshoot of turbulent heating is often noted in transition for supersonic and hypersonic ground test cases. Franko and Lele [3] identify overshoot in oblique breakdown cases as resulting from streaks increasing the wall-normal transport of thermal energy and streamwise momentum, and they report significantly less, if any, streamwise streaks in second mode dominated transition. Despite this, overshoot is often observed in flows where second mode demonstrates the greatest amplification up to the point of transition [4], and this fact highlights the difficulty in predicting transition-induced overshoot.

Accurate modeling of the transition region is a challenge for all varieties of RANS-based transition prediction. In transport-based transition model frameworks, the transition zone characteristics are often controlled by the same governing equations that control transition onset [5–7]. This makes the modification of the transition zone shape or extent difficult to accomplish without changing other aspects of the model's behavior. Transition prediction based on the coupling of CFD to hydrodynamics stability analysis presents an opportunity to advance the community's understanding of transition zone characteristics with respect to flow conditions and configuration. Because it does not rely on auxiliary transport equations to define intermittency, the relationship between the intermittency distribution in a CFD simulation and the resultant surface heating can be more easily isolated and studied. Moreover, ongoing efforts to advance coupled CFD-stability transition prediction [8–10] require the development of a robust intermittency model for hypersonic test cases. Previous analysis of coupled CFD-stability tools has used intermittency prescription based on the analysis of Narasimha [11] in conjunction with the Spalart-Almarras (SA) turbulence model [12], but this framework has been found insufficient for many hypersonic cases. Specifically, this method predicts more rapid transition than is observed in hypersonic experiments and is incapable of adequately including transition-induced overshoot of the turbulent heat transfer. This work outlines the development of a new intermittency modeling framework compatible with CFD-stability coupled analysis. This new approach is based on the modification of the SA turbulence model and the development of a correlation for intermittency distribution based on supersonic and hypersonic flight and ground test data.

The remainder of this manuscript is outlined as follows: first a discussion of the relevant background is presented. Next, the modifications to the turbulence model are described and the process by which the training database was developed is presented. Finally, the correlations are presented and a comparison of the predictions of the correlation to an independent test case is provided. Finally, a discussion of the present findings and future work is given.

# II. Background and Methodology

The present coupled CFD-stability analysis utilized NASA's OVERFLOW solver [13] and the LASTRAC stability analysis tool [14]. Coupled stability analysis using these tools has been demonstrated for a variety of flow scenarios, and a complete description is provided in Refs. [8, 9]. Previously, this method has been extended based on a data-driven correlation for transition N-factor in high speed flows [15], which allows for the application of this method to general hypersonic flows in ground test facilities. This previous correlation was developed by relating key parameters necessary to identify the transition N-factor to freestream flow parameters for a large number of test cases. The results of this analysis are detailed in Ref. [15]. The present study aims to utilize a similar approach to model the distribution of intermittency in the transition zone for high-speed cases in order to better estimate the integrated heat and pressure loads experienced by hypersonic flight systems.

Present RANS computations utilize a modified version the SA-neg turbulence model [12] that can better predict the finite length transition zone in hypersonic flows, in comparison with baseline SA version. Previous analysis pertaining to hypersonic flows has identified the improvement of the intermittency model as a key step to advancing the predictive capability of the method [16], and an example of the noted shortcomings is provided in Fig. 1. This figure shows the heat transfer and intermittency for a Mach 6 straight cone configuration in a conventional ground test facility. These previous analyses noted that, for some test cases, the point at which the heat transfer begins to increase can significantly lag the point at which the intermittency begins to rise. They additionally noted that, for these cases, heat transfer tends to rise more quickly in the RANS simulations than would be expected based on the corresponding experimental data. Moreover, this baseline approach does not make any consideration for transitional overshoot relative to the fully turbulent heat flux. As such, a new correlation for the prescription of intermittency in hypersonic flows must be developed to improve the method.

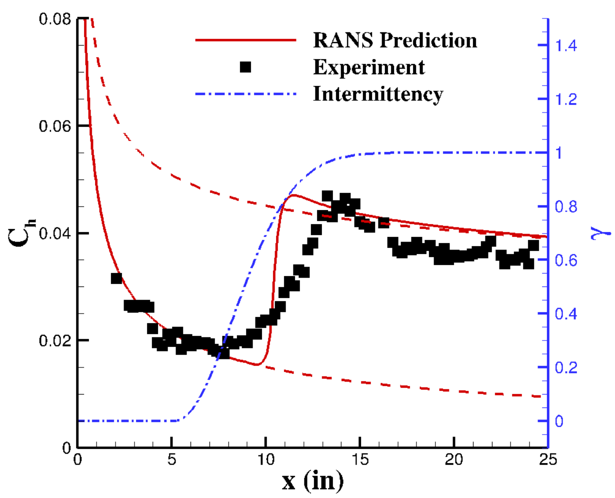


**Fig. 1 Heat transfer and intermittency distribution calculated via the baseline method described in Ref. [16]. Despite intermittency qualitatively aligning with the experimental transition zone, the resulting heat transfer increase occurs too far downstream and over too short a streamwise distribution compared to the experiment. Flow conditions correspond to a 7-degree half-angle sharp cone in the LaRC 20-inch Mach 6 ground test facility [4].**

To develop a relationship for predicting the necessary intermittency distribution across a set of conditions for high-speed flows, a number of individual tasks must be accomplished. First, a database of experimental test cases must be identified for which the experimental conditions and transition zone heat transfer distribution is known (or can be approximated if heat transfer data is sparse). Second, the intermittency to be applied to the CFD simulations must be appropriately parameterized. This parameterization must be able to reasonably approximate the experimental data with a relatively small number of parameters, as too many would make the subsequent tasks more difficult. Another crucial step involves the development of a methodology to identify the intermittency distribution parameters that would recover the experimental data for each individual test case. Given a sufficiently large database of appropriately parameterized test cases, the final step is to identify appropriate correlations for these parameters across flow and geometric conditions. This section outlines the process by which this correlation is developed using a selected set of canonical test cases from ground tests as well as flight experiments.

### A. Test Cases

One of the criteria for the selection of experimental data sets was that the data set must report not only the transition location, but the axial distribution of the surface heat transfer (or recovery factor, for nominally adiabatic wall cases). In the present work, data corresponding to experiments from the LaRC 20-inch Mach 6 tunnel [4], the Hypersonic Ludwieg Tube Braunschweig facility [17], the CUBRC LENS facility [18], the NASA Mach 3.5 Quiet Tunnel [19], AEDC Tunnel 9 [20, 21], and AEDC Tunnel B [22], along with data from the HIFiRE-1 flight test [23] and the NASA Langley Research Center's 1961 free flight experiment [24] are utilized in the development of the intermittency correlation. These test cases represent a variety of freestream conditions and facility/experiment type, and therefore it is anticipated that an intermittency model based on these canonical cases would reasonably capture the trends observed in general applications. Additionally, a straight cone configuration corresponding to an experiment conducted in the Von Karman Institute (VKI) Longshot facility [25] and virtual tunnel DNS of a Mach 8 straight cone simulated in a computational representation of the VKI tunnel are also included in this work. These final test cases are not used to develop the correlation but are instead held aside to evaluate the applicability of the correlation to an independent test case. Between 1 and 4 individual test cases are identified from each experimental reference, for a total of 26 test cases. Of these, 17 are used to in the training database for conventional ground test facilities, 4 are utilized for evaluating that correlation, and 5 are flight test cases which are considered separately from the ground test data.

All of the test cases included in this work are simulated with the HLLE++ upwind scheme [26] with symmetric successive over-relaxation (SSOR) [27] and the van Albada limiter [28] in OVERFLOW. These cases are simulated without a quadratic constitutive relation (QCR) or compressibility correction using meshes that have been previously found adequate for transport-equations based transition modeling applications [15].

**Table 1 Summary of experimental data sets included in the present correlation.**

| Facility | Mach Number(s) | Facility Type | Cone Half-Angle | Reference |
|---|---|---|---|---|
| LaRC 20-inch Mach 6 | 6 | Blow Down Tunnel | 5° | [4] |
| LaRC Mach 3.5 Quiet Tunnel | 3.5 | Blow Down Tunnel | 5° | [19] |
| AEDC Tunnel B | 8 | Blow Down Tunnel | Cone-Flare | [29] |
| AEDC Tunnel 9 | 10 and 14 | Blow Down Tunnel | 7° | [20, 21] |
| TU Braunschweig HLB | 5.9 | Ludwieg Tube | 7° | [17] |
| VKI Longshot Tunnel | 6.0 and 8.0 | Gun Tunnel | 7° | [25] |
| Virtual VKI Tunnel | 8.0 | Virtual Tunnel DNS | 7° | [30] |
| CUBRC LENS 1 | 7 to 10 | Shock Tunnel | 7° | [18] |
| HIFiRE-1 | approx. 5 | Flight | 7° | [23] |
| LaRC Free Flight | 3 to 4 | Flight | 10° | [24] |

### B. Turbulence Model Modification

In the course of this analysis, it became clear that the characteristics of the turbulence model can also pose a major obstacle to the adequate modeling of transition zone characteristics with coupled CFD-stability. Intermittency is conventionally introduced to RANS simulations via the production terms of the transport equations for the turbulence variables. This allows the intermittency to be prescribed or calculated via additional transport equations. However, this arrangement introduces an additional layer of abstraction between the intermittency distribution and the resulting distributions of relevant surface quantities, which represent the most important physical measures of the transition process. In CFD, the coupling of the intermittency to the turbulence model is effectively a transfer function that takes intermittency as an input and outputs a heat transfer or surface friction distribution. For the present application, a modification to the SA turbulence model is made to increase the level of control over the surface quantity distribution that can be exerted via the prescription of intermittency.

First, the SA-noft2 formulation of the SA model is used [**?** ]. Typically, modification of the production terms is used to influence a transition location. However, in the present work it was found that greater control of the intermittency zone characteristics could be achieved by modifying the eddy viscosity directly. Instead of multiplying the production terms by intermittency as is done in standard SA, the intermittency is included in the right hand side terms of the flow equations, where it multiplies eddy viscosity, so the Navier-Stokes equations would be modified such that the momentum equation is given as

$$\frac{\partial \overline{\rho}\widetilde{u}_i}{\partial t} + \frac{\partial \overline{\rho}\widetilde{u}_j\widetilde{u}_i}{\partial x_j} = -\frac{\partial \overline{P}}{\partial x_i} + \frac{\partial}{\partial x_j}\left[(\mu + \gamma\mu_T)\left(\frac{\partial \widetilde{u}_i}{\partial x_j} + \frac{\partial \widetilde{u}_i}{\partial x_j} - \frac{2}{3}\frac{\partial \widetilde{u}_k}{\partial x_k}\delta_{ij}\right) - \frac{2}{3}\overline{\rho}k\delta_{ij}\right], \tag{1}$$

and the other governing equations are similarly modified. The production terms of the SA model are not modified with intermittency, and so the present simulations utilize the standard SA-noft2 model. For brevity, the turbulence model is referred to simply as SA throughout this work, but it can be understood to be the SA-noft2 model. Put simply, this modification changes the turbulence model such that the of eddy viscosity predicted by the turbulence model influence on the flow is gated by the intermittency distribution. This modification has produced significantly greater range in the slope and extents of transition zone heat flux distributions than is possible to achieve via the standard formulation of SA. This formulation also allows for larger values of freestream eddy viscosity to be used, because the modification to the flow equations prevents the eddy viscosity from impacting the laminar boundary layer where intermittency is 0. While the destruction terms in the turbulence model are intended to remove eddy viscosity in the laminar portion of the flow, the present approach was found to maintain laminar flow with arbitrarily high values of freestream eddy viscosity. It is observed, particularly for ground test cases, that large values of freestream eddy viscosity allow for better agreement with experimental data because large freestream values of turbulent eddy viscosity increase the length of the transition zone and decrease the rate at which the surface heat transfer rises with increasing axial distance. Future work will examine the relationship between the freestream experimental noise level and the eddy viscosity prescribed in CFD to produce agreement between the two, but for the present model this parameter is not utilized as an independent variable.

### C. Computational versus Experimentally Observed Intermittency

Before presenting the parameterization of intermittency, it is necessary to clarify the difference between intermittency as discussed in a RANS context and the observed experimental quantity intermittency. The physical mechanism of natural transition in laminar flows is described in detail by Narashima and summarized here for completeness [31]. Transition occurs as the result of turbulent spots occurring in a narrow band at a particular streamwise position. These spots grow and merge over time, eventually resulting in a turbulent boundary layer. The process of transition via turbulent spot initiation and growth is visualized in Fig. 2. Intermittency in the context of experiments is a descriptive quantity that indicates the portion of time that the flow at a particular point in space is turbulent, and thus cannot exceed a value of 1. For the purposes of this work, the true, physical intermittency which describes the relative fraction of time flow is turbulent at given point in space is denoted as $\Gamma$. In all flows $0 \leq \Gamma \leq 1$, and Fig. 2 illustrates the growth of $\Gamma$ in a flow. In the context of RANS simulations, which are time-averaged, intermittency is a parameter that seeks to replicate experimentally observed transition characterizations. This prescribed or computational intermittency is denoted here as $\gamma$, and attempts to mimic the transitional characteristics of a flow in the context of time-averaged CFD.

Both the physical $\Gamma$ and computational parameter $\gamma$ are equal to 0 in laminar portions of the flow, but the two quantities define slightly different things. $\Gamma$ is observed directly in experiments, whereas $\gamma$ is imposed in computations to replicate (insofar as is possible) the flow parameters of interest which result from transition, all the while preserving the stability and well-posedness of a simulation. Therefore, $\gamma$ takes on properties that are different from the experimental quantity, $\Gamma$, it seeks to reproduce. Computational intermittency must be defined at all points in a transitional RANS flow, takes a value of 1 at the freestream to prevent negative impacts on the performance of the transition and turbulence models, and can take a value greater than one to increase the local impact of the turbulence model it modifies. Therefore, the present intermittency model can allow the computational parameter $\gamma$ to assume values greater than one in order to replicate experimentally observed overshoot of turbulent heat transfer.

### D. Intermittency Prescription

In order to develop a correlation to predict the intermittency distribution as a function of flow and geometric conditions, the intermittency distribution is first parameterized. Based on the previous works of Narashima et al. [31] the parameterization chosen for this work is a Gaussian distribution. This approach has been modified to accommodate the possibility of overshoot, as in,

$$\gamma = (1 + C_{ov})(1 - exp(-\eta_1\zeta_1^2)) - C_{ov}(1 - exp(-\eta_2\zeta_2^2)), \tag{2}$$

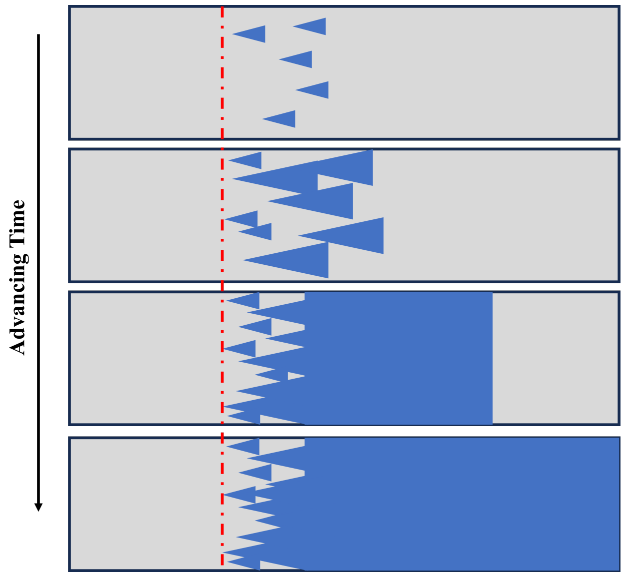


**Fig. 2 Visual representation of laminar-turbulent transition via the generation of intermittent turbulent spots. This figure is adapted from Ref. [32] for demonstration purposes.**

where

$$\zeta_1 = \frac{x - x_{onset}}{x_{os} - x_{onset}} \tag{3}$$

and

$$\zeta_2 = \frac{x - x_{os}}{x_{turb} - x_{os}}. \tag{4}$$

In these equations, $C_{ov}$ is the overshoot parameter, $\zeta_1$ and $\zeta_2$ are nondimensionalized transition zone coordinates, and $\eta_1$ and $\eta_2$ are exponents that dictate the rate of increase or decrease of $\gamma$. The referenced streamwise positions, $x$, $x_{onset}$, $x_{os}$, and $x_{turb}$ are the local streamwise position, the streamwise location of the onset of transition (i.e. the beginning of the transition zone), the streamwise position at which the maximum overshoot occurs, and the location at which the transition zone intersects the fully turbulent zone (i.e. the end of the transition zone). For cases with no overshoot, $x_{os} = x_{turb}$. This parameterization maintains the conventional Gaussian intermittency distribution accepted in the literature [31] while allowing for intermittency distributions of varying width, overshoot extent, and overshoot location. Limits are placed on some parameters so that Eq. 2 converges to a simple (no-overshoot) Gaussian distribution for cases without overshoot. An overshoot parameter value of $C_{ov}$=0 corresponds to the no-overshoot case in which $\gamma$ increases monotonically to a maximum value of 1. The exponents $\eta_1$ and $\eta_2$ are also limited to $0.01 > \eta > 1.5$, as larger or smaller values tend to produce intermittency distributions that yield unphysical heat transfer results and/or cause the CFD simulation to diverge.

Parameters $C_{ov}$, $\eta_1$, and $\eta_2$ from Eq. 2 are individually tuned for each training case via automated, gradient-free root-finding algorithm that seeks to minimize the more between the predicted surface load distribution (heat transfer in all sufficiently non-adiabatic cases and ... for the near adiabatic cases?) and the measured data. The measured distributions are adjusted to align with the CFD predictions in fully laminar and fully turbulent regions.. Performing this process for each test case provides the intermittency parameters necessary to reproduce transition zone characteristics across a broad range of conditions. This database is to be used to develop correlations between the intermittency parameters defined in Eq. 2 and the freestream and geometry parameters of the test cases. In practice, $x_{onset}$ would be calculated by a separate correlation, such as the one identified in previous works by the authors [15]. However, to ensure that the data used to train the present correlation is as accurate as possible, the present exercise allows the black-box optimizer to determine $x_{onset}$ with the goal of providing the most accurate training database as possible for the current study. This approach also prevents interdependence between the present model and the previous results, allowing either model to be replaced or updated in the coupled stability analysis protocol as improvements are made to the method in future work. Additinally, previous methods, such as the intermittency model used for low-speed flows, have found that initiating the growth of $\gamma$ slightly upstream of the intended transition location can increase the agreement between the modeled transition and the experiment. Allowing the optimizer control over the placement of $x_{onset}$ enables the present high-speed model to account for the possibility that the intermittency for a given test case should begin to rise upstream of the intended onset transition as identified by the surface heat transfer.

The goal of the present study is to develop a robust and broadly applicable, closed form correlation for the accurate of estimation of intermittency parameters (and therefore transition zone extent and shape) purely as a function of easily available freestream flow, freestream turbulence, and geometric information.

### *1. Identification of Intermittency Parameter Values*

The goal of the current study is to develop a model for the prediction of the intermittency parameters for high-speed flows based on flow information and potentially the transition N-factor. Before the chosen test cases can be examined for the purposes of constructing such a model, however, the values of these parameters necessary to recover the experimentally observed transition zone characteristics must be found. This task is highly nontrivial because the intermittency parameters for a given test case cannot be observed directly. Instead, the efficacy of a set of trial parameters can be evaluated by comparing the transition zone characteristics they produce when applied to a RANS simulation to the experimental results corresponding to the same conditions. Therefore, the identification of the intermittency parameters is a black-box problem whose goal is to find the input (intermittency parameters) that minimize the error between their corresponding output (CFD results) and a reference value (the experimental data).

To solve this problem, a gradient-free error minimization routine was developed to identify the parameters that produc e the best agreement with the experimental Stanton number distribution in the transition zone. This algorithm produces candidate inputs based on a Latin hypercube distribution of the five intermittency parameters within specified bounds, then conducts a RANS simulation of the test case based on combinations of those parameters. The error between the experimental data and computational results is calculated in terms of Stanton number, and then the bounds of the grid search are reduced by 50% centered on the best-performing parameters from the previous iteration. This approach provides robustness in the determination of the intermittency parameters, and the convergence and outcome of each test case was evaluated to ensure the final parameters produced satisfactory agreement with the underlying experimental data. To ensure reasonable results, some specific limitations were placed on the allowable values of the intermittency parameters. These were that $x_{onset} < x_{os} < x_{turb}$, $\eta_{1,2} > 0$, and $C_{ov} > 0$. For each test case, the algorithm was utilized for 10 iterations with 20 sets of parameters utilized in the grid search for each iteration. In total, each test case considered in the training database was simulated 200 times to identify the best-performing intermittency parameters for that case.

Experimental data in transition studies are often sparse and/or somewhat noisy. Because of this, it is necessary to perform some processing on the experimental data to ensure that a consistent means of evaluating agreement between the experiment and computations and to ensure that uncertainty in the experimental data away from the transition zone does not influence the determination of the intermittency parameters. To address these concerns, a reference curve was created for each test case that represents the transition characteristics of the experimental data and recovers the laminar and turbulent values expected from CFD in the regions of the flow away from the transition point. Reference curves were created for each test case by combining fully laminar and fully turbulent CFD profiles with Gaussian fits of the transition region. An example is provided in Fig. 3 9(a). As this figure shows, the reference curve-based approach removes scatter from the experimental data, clarifies the ambiguity of sparsely sampled experimental data, and ensures that the reference curves exhibit the expected behavior in the laminar and turbulent regions of the flow. For some cases, such as the HIFiRE-1 flight test data, the experimental data is particularly sparse, and so reference curves are defined based on engineering best-judgment where the data itself is insufficient to fully clarify the transition zone characteristics. These reference curves, rather than the experimental data themselves, are used to evaluate the error between the CFD and experiment for each case. Fig. 3 (b) and (c) demonstrate the convergence of the black-box algorithm for the determination of the exponent $\eta_1$ for one of the AEDC Tunnel 9 cases. In the evaluation of agreement between the CFD and reference curve, the overall error is calculated as the mean of the absolute value of the difference between the local Stanton number at each grid point in the candidate CFD result and in the reference curve, as in the L1 norm:

$$E = \frac{\sum_{N_p} |C_{h,cfd} - C_{h,ref}|}{N_p}. \tag{5}$$

The error was evaluated across the entire surface of the geometry in each case. Because of this, the value of the overall error is relatively small even for cases for which visual agreement between the CFD and reference is poor (because the laminar and turbulent regions still have very low local error, even if the transition zone does not). This approach was taken to eliminate the possibility that candidate parameter sets might somehow produce good agreement in the transition zone, but negatively impact the quality of the solution in the laminar or turbulent zones. The relative error could not be entirely eradicated in these cases, however, and this is observed to be a result of several phenomena. First, for cases with overshoot of the turbulent flow, the experimental data tend to have sharper 'peaks' in their surface heating distribution than are possible to achieve with the present turbulence model. The second, and more common phenomenon was transitional heating hysteresis, where, regardless of the presence or absence of overshoot, the heat transfer just downstream of transition tends to be slightly higher than the equivalent fully turbulent case (on which the reference curves are based). Despite these observations and the relatively small differences in the overall error between iteration 1 and the final iteration in most cases, each case converged to a set of transition parameters that produced good visual agreement with the experimental data.

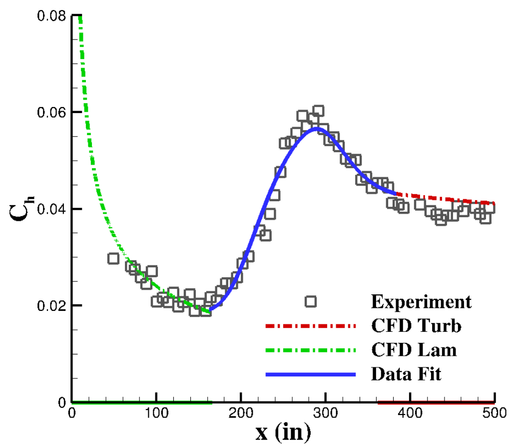


(a) Reference for LaRC Mach 6 Cone [4]

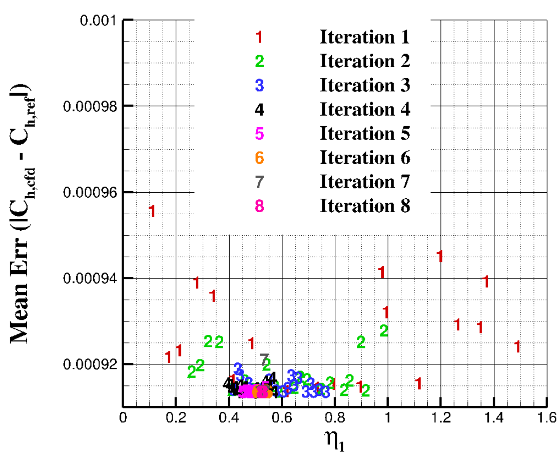


(b) Convergence of $\eta_1$, Mach 14 cone

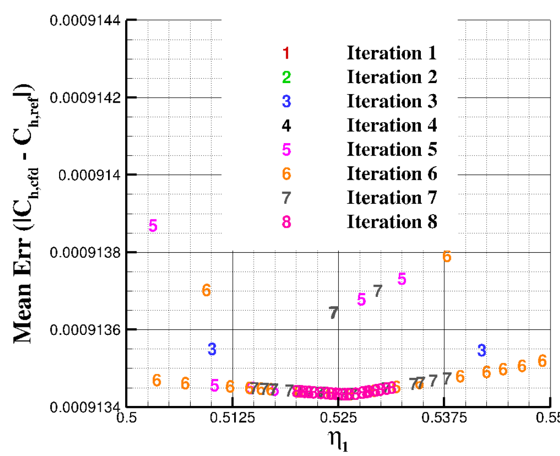


(c) Convergence of $\eta_1$ Mach 14 cone zoomed in

**Fig. 3 Visual representations of the process by which the intermittency parameters for a given test case were obtained. Subfigure (A) shows and example of the curve fits utilized by the black-box algorithm, in this case for a LaRC Mach 6 [4] cone. Subfigures (b) and (c) depict the reduction in error with successive iterations of the black-box algorithm and the convergence of the intermittency exponent $\eta_1$.**

*2. Connection to Turbulent Spot Spreading*

Equations 2 through 4 represent the expected form of the intermittency distribution for general hypersonic flows with overshoot. While a model for these parameters is not available in the literature, examination of experimental data has been conducted in the literature to identify the turbulent spot initiation rate in ground test facilities [31–33]. These studies differ from the present model in several ways. First, these studies concern experimental intermittency, $\Gamma$, and so they do not make any consideration for overshoot of turbulent heating. Second, these studies take the value of $\eta_1$ to be a constant equal to 0.412. This has been demonstrated to be an appropriate simplification when examining experimental intermittency [31] for cases with small pressure gradients, but it has been demonstrated not to yield good results when utilized to predict computational intermittency for coupled RANS-stability analysis in high-speed flows [9]. Based on this simplification and other relationships outlined in Ref. [32], these studied are able to relate the intermittency zone width directly to the turbulent spot generation rate. Therefore, while these previous studies are not suitable to ascertain a model for the parameters in equations 2 through 4 directly, they can provide useful insights into the expected outcomes of the present study and the expected independent variables to consider. Ref. [33] examines a large number of test cases to evaluate the turbulent spot generation rate as a function of freestream variables. A number of trends are observed in Ref. [33] thare relevant to the present work.

While the present parameters cannot be expressed directly in terms of an equivalent turbulent spot generation rate because of the difference in the number of free parameters in each approach, larger turbulent spot propagation rates correspond to a more rapid transition from laminar to turbulent, and therefore a larger value of $\eta_1$ and a smaller value of the nondimensional transition zone extent, assuming, as is the case in the framework of Ref. [32] that overshoot is not a factor, and so $C_{ov}$, $x_3$, and $\eta_2$ are not relevant to the flow. Ref. [32] demonstrates that the turbulent spot generation rate increases monotonically with increasing unit Reynolds number and increasing wall-to-stagnation temperature ratio. Spot initiation rate increases initially with increasing edge Mach number but begins to decrease with edge Mach numbers above approximately 8.5. Based on these observations and observations made directly from the present training data, a correlation to approximate the experimental transition behavior for the training database is developed.

# III. Results

The automated black-box analysis has been conducted on all 22 training cases included in the present work in order to determine the intermittency parameters necessary to achieve agreement in transition behavior between the experiments and the CFD. All of these test cases utilize the modified version of the SA turbulence model discussed above, and the results, corresponding to CFD simulations using tuned parameters identified by the automated process, are presented for four of these cases in Fig. 4. In these figures, the upper and lower dashed lines represent the fully turbulent and fully laminar solutions calculated in OVERFLOW. The turbulent reference curves utilize the unmodified version of the SA turbulence model, and for the case of a fully turbulent boundary layer, the present modification was found to have no influence on the predicted heat transfer. This figure demonstrates that the automated procedure is able to produce fairly good agreement with the experimental data. It is notable that the fully turbulent solutions calculated using the SA-neg turbulence model sometimes predict heat transfer rates greater than those observed in the fully turbulent experimental data, notably the CUBRC Lens and HLB data shown in Fig. 4 (c) and (d). This discrepancy is generally small and is independent of the intermittency distribution. This phenomenon is observed in multiple places in the literature as well as the present work [4, 5, 25, 34], and is discussed in detail for instances where it is relevant to the interpretation of the present results.

## A. Intermittency Model

Based on the training database, correlations have been developed to predict the intermittency distribution for hypersonic flows over canonical hypersonic configurations. These correlations are developed based on conical configurations at 0-degrees angle-of-attack where transition is dominated by Mack's first and second modes. This correlation is developed by comparing the parameters of the ideal intermittency prescriptions (identified through the error minimization algorithm) to the freestream parameters of each test case in the training database. The specific parameters of interest are the freestream Mach number, the freestream Reynolds number, the wall-to-stagnation temperature ratio, and the transition onset location.

The majority of the data utilized in the development of the present correlation is for ground test cases of canonical straight-cone geometries. This type of geometry represents a majority of the experimental data available in the literature for the development of this work. Oone database of Mach 3.5 cases examined under quiet flow is also included here [19]. The training and evaluation of the correlation for ground test cases is performed using 21 individual test cases (17

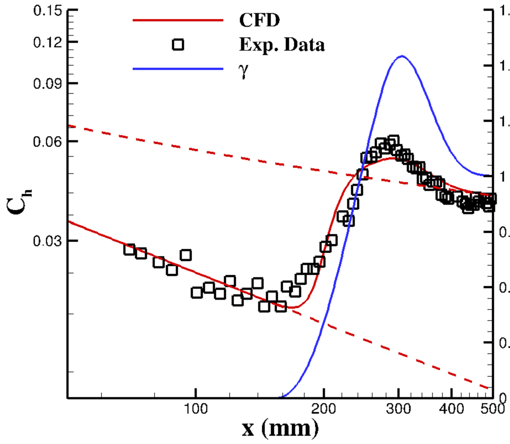


(a) LaRC Mach 6 Cone [4]

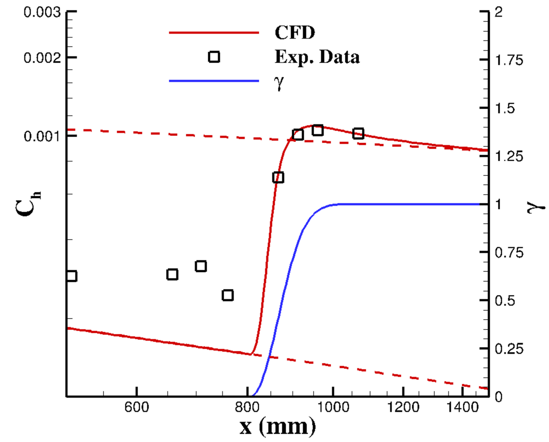


(b) HIFiRE-1 Flight Data [23]

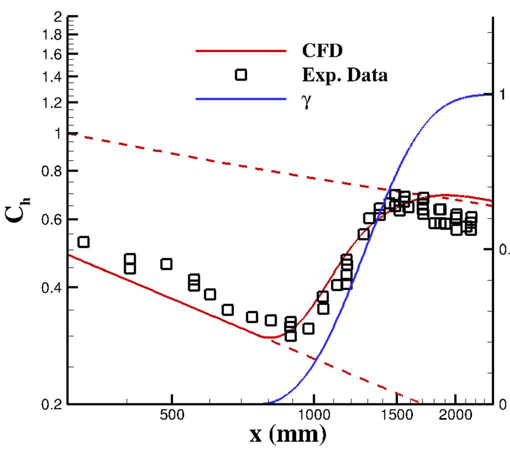


(c) CUBRC Mach 10 Cone [18]

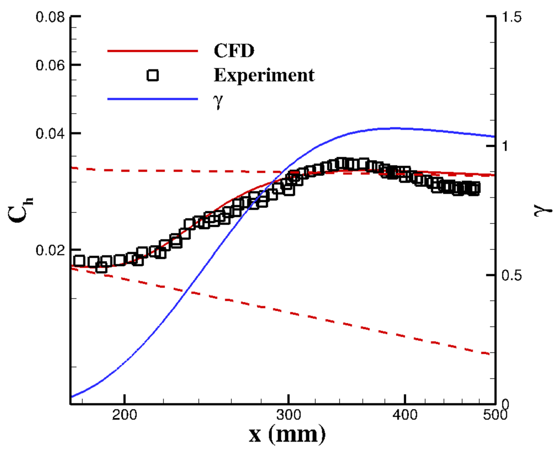


(d) DLR Mach 5.9 Cone [17]

**Fig. 4 Intermittency values found to minimize experimental error for representative test cases from the training database. Itermittency parameters are found via the root-finding algorithm.**

for training, 4 for evaluation), and 5 flight test cases utilized to analyze the trends in intermittency parameters in the context of flight tests and develope a preliminary correlation for flight data.

In developing this correlation based on the assumption of a known transition onset location, the distance values required by Eqs. 2 through 4 are nondimensionalized in terms of freestream Reynolds number as,

$$x_{onset} = \frac{Re_{onset}}{Re_\infty}, \qquad x_{os} = \frac{Re_{os}}{Re_\infty}, \qquad x_{turb} = \frac{Re_{turb}}{Re_\infty}. \tag{6}$$

Because $x_{onset}$ can be estimated independently of the intermittency prescription [15], it is treated as known for this analysis. Therefore, the number of distance parameters that must be estimated can be reduced by defining the width parameters

$$\Delta Re_1 = Re_{os} - Re_{onset}, \qquad \Delta Re_2 = Re_{turb} - Re_{os}. \tag{7}$$

After this consolidation, the parameters that must be found are the nondimensional width of the pre-overshoot and post-overshoot regions, $\Delta Re_1$ and $\Delta Re_2$, the two exponents, $\eta_1$ and $\eta_2$, and the overshoot parameter $C_{ov}$. Additionally, for cases where overshoot is not observed, and therefore $C_{ov} = 0$, the two parameters that govern the intermittency distribution downstream of the overshoot peak, $\eta_2$ and $\Delta Re_2$ have no influence over the resulting intermittency distribution. A correlation for these parameters as a function of the freestream flow parameters (i.e. Mach number, Reynolds number, and wall-to-freestream temperature ratio) and the transition onset location has been developed. The use of global parameters rather than the local flow conditions is a practical compromise to reduce the overall complexity associated with the implementation of the intermittency model developed here. The predictions of a model developed this way may not necessarily generalize beyond the conditions represented in its training database. To minimize the negative impact of extrapolation outside of the training database, the database is chosen so as to include a diverse set of flow conditions and cone geometries (subject to the availability of experimental reference data) and the model is evaluated using unseen test cases both within and outside of the training database conditions.

*1. Correlation based on Straight-Cones in Ground Test Facilities*

The first correlation presented is that for straight cones in ground test facilities. This correlation is also evaluated against an independent set of test cases to ensure that overfitting has not occurred. This correlation is developed based on test cases from 6 ground test facilities and evaluated based on data from a separate facility. Before presenting the correlation itself, it is beneficial to discuss trends in the experimental data that can be observed directly from their examination.

It can be observed in the available data that significant overshoot is only observed within a handful of cases, notably those corresponding to the 20-inch Mach 6 tunnel experiments [4], the VKI experiments and DNS [25], the HLB experiments [17], and the AEDC tunnel B experiments [22]. These cases have freestream Mach numbers high enough to be dominated by the second mode, but not so high as to eliminate the relevance of the first mode entirely. This supports the findings of Franko and Lele [3], who observed that heat transfer overshoot was most pronounced in the case of oblique first mode breakdown in their DNS of a hypersonic flat plate boundary layer. The implications of this for the present correlation are twofold. First, the number of cases for which overshoot can be observed and used in the training database is small, and second the correlation for overshoot should include some gating mechanism to exclude cases with high Mach number, low Mach number, and small wall-to-stagnation temperature ratios.

The approach to the development of the correlation begins with the development of a baseline correlation for straight cone configurations with zero pressure gradient. These correlations were developed manually by identifying variable groupings which produce good visual collapse of the data based on the expectations established from the previous literature [32]. These correlations were then adjusted by tuning the individual constants so as to minimize the mean error between the collapsed data and a least-squares fit of the experimental data based on the manually determined independent variable groupings. A small number equations, those for the overshoot parameters were chosen based on different criteria, and these exceptions are discussed as they appear. The straight cone correlation for $\Delta Re_1$ takes the form,

$$\Delta Re_1 = 1.9571 \times 10^{-24}\alpha_{t,1}^3 - 1.55034 \times 10^{-13}\alpha_{t,1}^2 + 1.5113 \times 10^{-3}\alpha_{t,1} - 6.6725 \times 10^3, \tag{8}$$

where

$$\alpha_{t,1} = Re_\infty M_\infty^{3.43}(T_w/T_{tot})^{0.42}. \tag{9}$$

For adiabatic cases, the laminar recovery factor of 0.84 is assumed for surface temperature. Because $x_1$ is a known quantity, and $Re_1$ can be calculated based on freestream parameters, it can be used as an input for subsequent correlations. For cases with high Reynolds number and high Mach number, the value of $\Delta Re_1$ is limited to $2.25\times10^6$. The first exponent is then calculated as

$$\eta_1 = 0.0034[(\Delta Re_1/Re_{onset})^{1/2} Re_\infty M_\infty^2 (T_w/T_{tot})]^{0.28198} \tag{10}$$

and the overshoot parameter is calculated as

$$C_{ov} = \max[\min[1.0, 3.0047 \times 10^{-10}(Re_\infty M_\infty^3) - 0.5907], 0.0], \tag{11}$$

for cases which satisfy

$$3.5 < M_\infty < 10.0. \tag{12}$$

For cases outside of this domain, $C_{ov} = 0$. This limiter seeks to eliminate cases without sufficient amplification of the 1st mode to induce overshoot, following the findings of Franko and Lele and consistent with the trends observed in the present database. Future work will seek to combine the present model with previous work relating to the prediction of critical N-factors for second mode instabilities and establish a relationship for determining the possibility of overshoot in a given test case based on the ratio of the first and second mode N-factor at the point of transition. Such an approach could be expected to be slightly more robust than the present limiter in that it could also capture the effects of other features such as nose bluntness and wall-to-freestream temperature ratio.

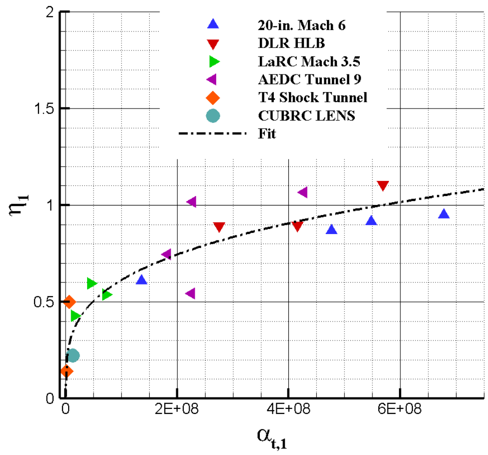


(a) Fit for $\eta_1$

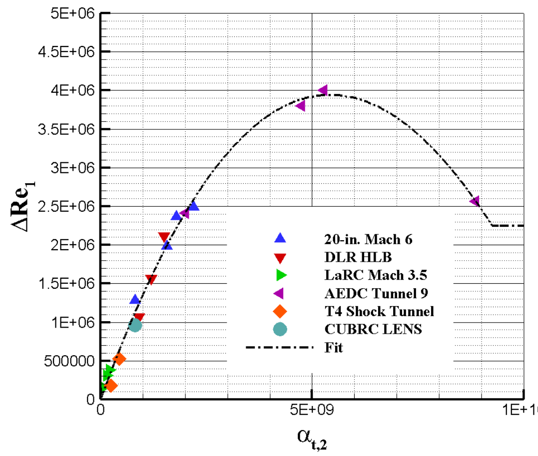


(b) Fit for $\Delta Re_{12}$

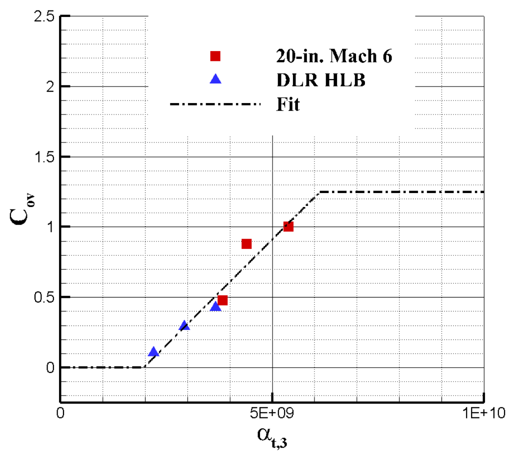


(c) Fit for $C_{on}$

**Fig. 5 Visualizations of the intermittency parameters, $\eta_1$, $\Delta$Re$_1$, and $C_{ov}$ which govern the intermittency curve exponent, intermittency zone width, and degree of overshoot. Curves reflect limiters imposed to manage the effects of extrapolation beyond the current database for training.**

The collapse of the data used to develop Eqs. 8 - 12 are provided in Fig. 5. It is observed that the correlation for $\eta_1$ exhibits more scatter than the other two. The predictions of the present model were found to be less sensitive to this parameter provided that $\Delta Re_1$ is appropriately predicted. For example, Fig. 6 highlights the two cases with the largest overestimation and underestimation of the value of $\eta_1$ determined by the algorithm. These two cases correspond respectively to the CUBRC LENS case (where the correlation predicts $\eta_1$ = 0.412 instead of 0.211) and one of the AEDC Mach 10 cases (where the correlation predicts $\eta_1$ = 0.879 instead of 1.016). As can be seen in Fig. 6, provided adequate estimation of $\Delta Re_1$, adequate estimation of the transition zone characteristics is still possible. For the Tunnel 9 case visual agreement with the experiment is observed in both cases, and, for the CUBRC LENS case, transition-induced heat transfer rise occurs slightly earlier than in the experiment but the transition zone slope still approximates the experiment.

The final two parameters, $\Delta Re_2$ and $\eta_2$ are only applicable for cases with a significant overshoot, and therefore only those cases can be used to tune the correlations for these parameters. Based on this subset of the training database, the

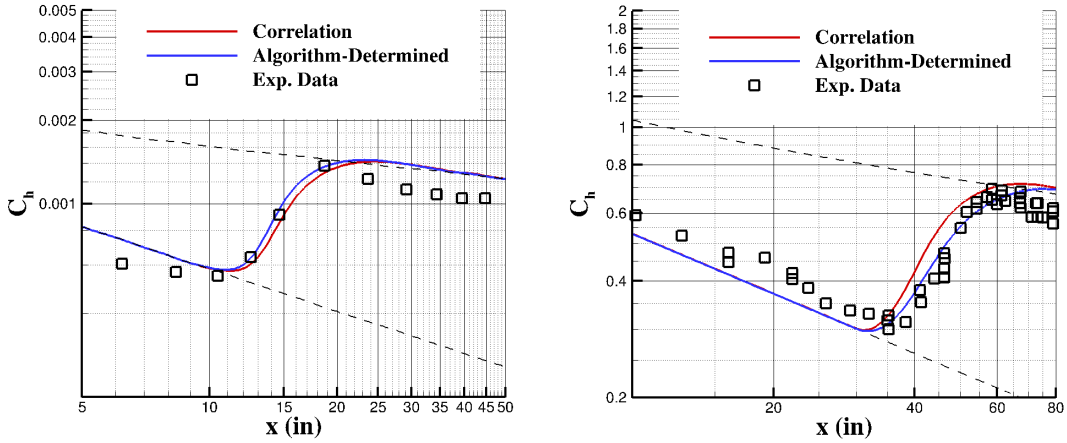


(a) AEDC Tunnel 9 (c) CUBRC LENS

**Fig. 6 Surface heat transfer profiles calculated using $\eta_1$ values calculated via the black-box algorithm as compared to those calculated with Eq. 10 for the two cases for which these two values showed the largest differences. The two cases are the AEDC Tunnel 9 Mach 10 cone, and the CUBRC LENS Mach 10 cone.**

final two parameters are calculated as

$$\frac{\eta_2}{\eta_1} = \tanh[2.464 \times 10^{-7}(Re_\infty - 1545891)] + 1.02, \tag{13}$$

and

$$\Delta Re_2 = \Delta Re_1. \tag{14}$$

These relationships are visually demonstrated in Fig. 7. A minimum permissible value of $\frac{\eta_2}{\eta_1} = 0.02$ is recommended to eliminate the possibility that, for some low Reynolds number cases with overshoot, unreasonably small values of $\eta_2$ might otherwise lead the model to overpredict the turbulent heat transfer for a significant portion of the domain. This limit is enforced implicitly via the use of the hyperbolic tangent fit. Notably, Eq. 14 is the only relationship in the present model not based on a least-squares fit, and was instead chosen to simplify the model by reducing the number of quantities that must be calculated, and because the simple equivalence produces good predictions for most test cases.

In addition to Eq. 9, additional shorthand nomenclature is introduced to clarify the visualizations included in this work. These are

$$\alpha_{t,1} = (\Delta Re_1/Re_{onset})^{1/2} Re_\infty M_\infty^2 (T_w/T_{tot}), \tag{15}$$

and

$$\alpha_{t,3} = Re_\infty M_\infty^3, \tag{16}$$

for ground test cases and

$$\alpha_{1,f} = Re_\infty M_\infty^{1.55}, \tag{17}$$

and

$$\alpha_{2,f} = (\Delta Re_1/Re_{onset}) M_\infty^{3.8} \tag{18}$$

for flight cases.

*2. Correlation based on Straight Cones in Flight*

Evaluating the intermittency characteristics of flight test experiments for supersonic and hypersonic flight test cases can be a challenge due to the lack of available data. This can present a problem both in terms of the number of reference test cases available– there have been significantly fewer flight test experiments than ground test campaigns for hypersonic flows, and in terms of the ability of a data set to be used in the development of a correlation– flight test data often has high associated uncertainty. Despite these challenges, two flight test campaigns are examined here in order to

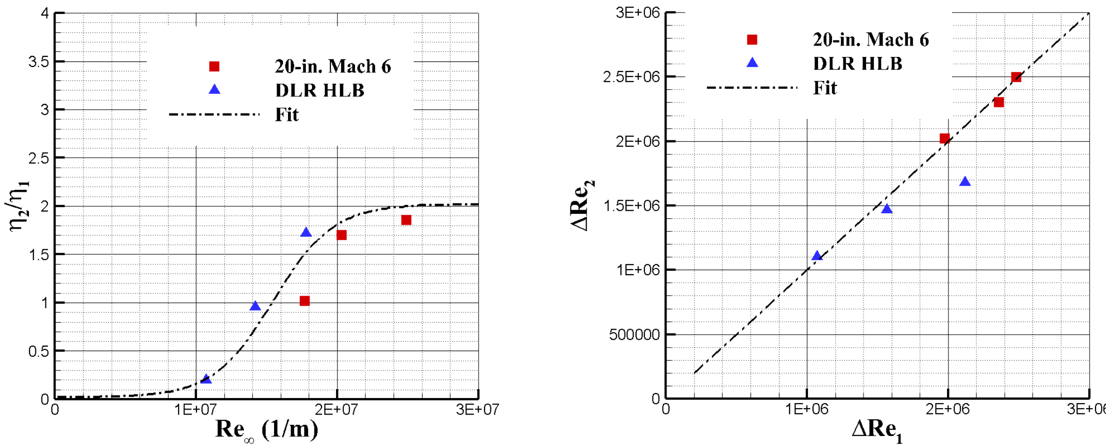


(a) Fit for $\eta_2$ (b) Fit for $\Delta Re_2$

**Fig. 7 Visualizations of the secondary intermittency parameters, $\eta_2$ and $\Delta\mathrm{Re}_2$, that are only valid in cases with significant overshoot of experimental heat transfer.**

develop a baseline correlation for flight test cases. One of the goals of this exercise is to develop an understanding of the differences between the intermittency distributions between ground and flight test cases. Neither of the two flight test campaigns exhibited overshoot, although uncertainty in the experimental data means that overshoot could be inferred if preferred. The approach taken in the present study was to infer overshoot only in cases where the evidence for it is clear. Based on the limited data available data, the correlations for the flight test cases are found to be,

$$\Delta Re_1 = \min[\max[0.568(Re_\infty M_\infty^{1.55}) + 1.0609 \times 10^7, 1 \times 10^5], 1.75 \times 10^7] \tag{19}$$

and

$$\eta_1 = \min[\max[-0.0266[(\Delta Re/Re_{onset})M_\infty^{3.8}] + 1.6545, 0.1], 1.25]. \tag{20}$$

These relationships are shown in Fig. 8

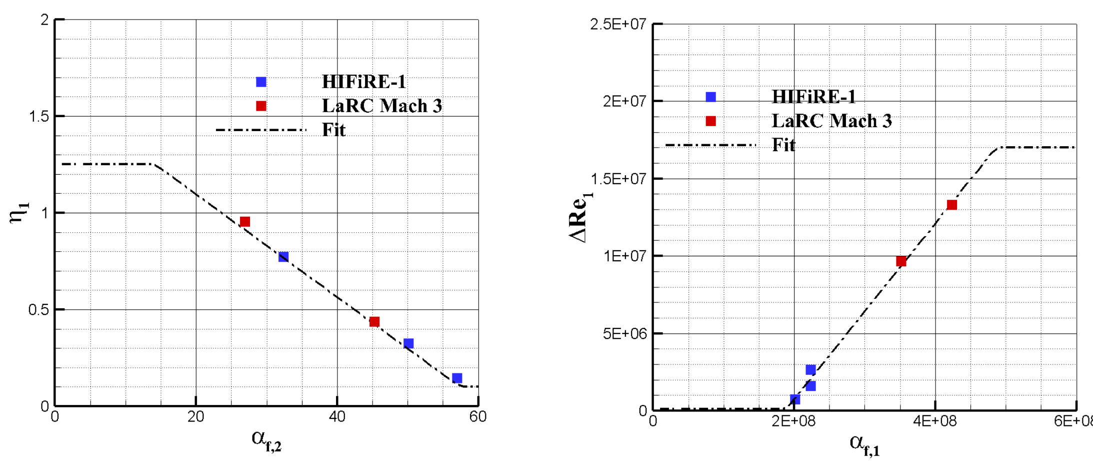


(a) Fit for $\eta_1$ (b) Fit for $\Delta Re_{12}$

**Fig. 8 Visualizations of the preliminary correlation for flight test cases based on the HIFiRE-1 and LaRC free flight experiments. For the preliminary correlation, potential turbulent overshoot of experimental heat flux is not considered.**

It is notable that the behavior observed for $\Delta Re_1$ is similar to that observed in the same Mach number range for the ground test cases. In both, $\Delta Re_1$ is found to increase with increasing Mach number and Reynolds number. However, the exponent parameter, $\eta_1$, displays the reverse relationship to that observed in the ground test cases. In the ground test cases, $\eta_1$ is found to increase with increasing Mach number and Reynolds number, whereas for the flight data it is found to decrease with these parameters. Because there is less data available for flight tests, the preliminary correlation for flight test cases utilizes limiters on both quantities to ensure reasonable predictions outside of the training database.

It is possible that the intermittency parameters for general applications could be calculated using a single correlation by including either the N-factor at transition or the freestream disturbance level as inputs to the correlation. For Mack's second mode, the transition N-factor in conventional ground test facilities is usually approximately 4 [15] whereas investigation for flight test cases has found transition N-factors closer to 15 [35]. If the same trends hold for Mack's first mode, this could provide a basis for such a combination. It is also noteworthy that the intermittency parameters for the HIFiRE-1 test case are similar to those for cases with similar Mach number, but the LaRC free flight data exhibit transition zone widths much larger than any other test case included. This suggests that attempting to divide the training database on the basis of which mode is more amplified at transition rather than based on freestream noise level may yield further insights. Both of these possibilities will be explored in future work that plans to explore the N-factor for first and second mode at the transition onset location as inputs to a potential improved correlation.

*3. Evaluation Cases*

The efficacy of the correlation is evaluated by applying its predictions for an independent set of test cases. These are the Mach 6 straight cone experiments of Grossir et al. [25] and the Mach 8 straight cone case corresponding to the virtual tunnel DNS of Schaubb et al. [30]. Each evaluation case corresponds to a different freestream Reynolds number, ranging from $1.22\times10^7$ to $2.71\times10^7$/m. Similar to the training database, the transition onset location is presumed to be known in these cases. Based on this information, the intermittency parameters are evaluated with the intermittency correlations from Eqs. 8 - 14 and the resulting simulation is used to predict the heat transfer profile in the transition zone. The results of these test cases are presented in Fig. 9. Observe that the agreement with the experimental data is significantly improved as compared to the baseline intermittency relationship corresponding to the methodology outlined in Ref. [9]. The experimental data exhibit a tendency to decrease more rapidly than is predicted by CFD in the fully turbulent region, and so the agreement between the CFD and experiments tends to decrease downstream of transition. This phenomenon was observed in some instances in the training database as well, including for cases without the modification to SA used in the present case. These discrepancies are likely due to limitations of the underlying RANS model for hypersonic flows and/or due to the relatively modest length of the turbulent region on the experimental model. Therefore, this behavior cannot be corrected via a modification to the transition region, and it is not of focus in the present work. Discounting this phenomenon, the agreement between the experimental data and CFD is found to be qualitatively good in all cases, including those with overshoot. Some degree of overshoot is predicted in all four of these evaluation cases, although for the Fig. 9(c), the $Re_\infty = 1.81\times10^7$/m case, the flow reaches the end of the cone before overshoot occurs. For the case that shows the largest disagreement between the experiment and predicted heat transfer values, the $Re = 2.71\times10^7$/m case, agreement could be improved by slightly increasing the transition zone length and increasing the transition zone exponent $\eta_1$. The unit Reynolds number of this case is larger than any other case included in the training database, and so it is not surprising that this case also corresponds to the largest error of the evaluation cases. It is also noteworthy that the virtual tunnel DNS case predicts substantial overshoot, and the heat flux is still substantially larger than the reference turbulent value at the end of the domain simulated for this test case. The heat transfer calculated based on the DNS result is shown to converge to the van Driest solution at approximately x = 500 mm in Ref. [30], and the fully turbulent SA solution is found to under-predict the turbulent heat transfer in the same region as compared to the DNS. The present transitional solution is found to produce good agreement with the DNS, and while it does not reach the baseline turbulent value by the end of the domain, the difference between the heat transfer calculated by the correlation and the DNS is small.

## IV. Conclusions and Future Work

Previous work has demonstrated the feasibility of laminar-turbulent transition prediction in canonical hypersonic flows using coupled CFD-stability analysis [9]. However, despite the potential of this method, the hypersonic regime presents specific challenges for the method which are not present for lower-speed flows. Namely, the critical N-factor for transition and intermittency evolution across the transition zone have been thoroughly studied for subsonic and transonic flows, and models identified from the existing literature have been shown to produce good results at low-speeds

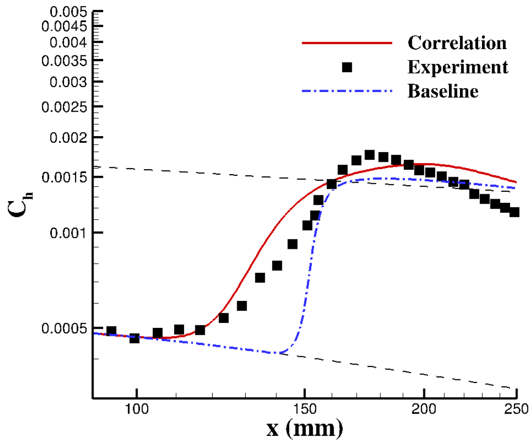


(a) M= 6.0, Re = 2.71×10$^7$

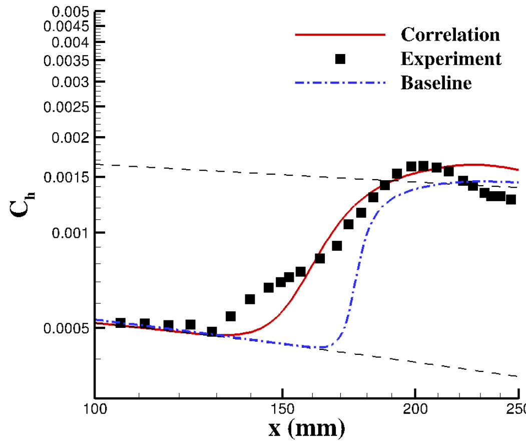


(b) M= 6.0, Re = 2.28×10$^7$

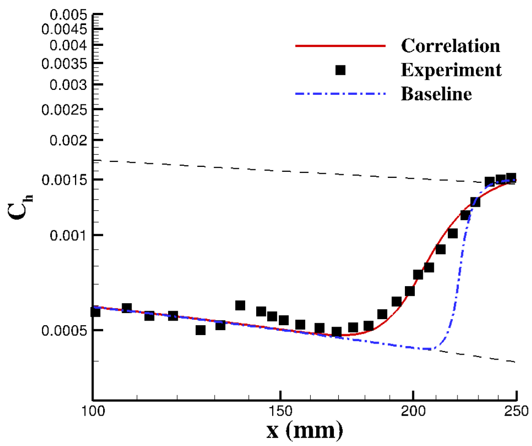


(c) M= 6.0, Re = 1.80×10$^7$

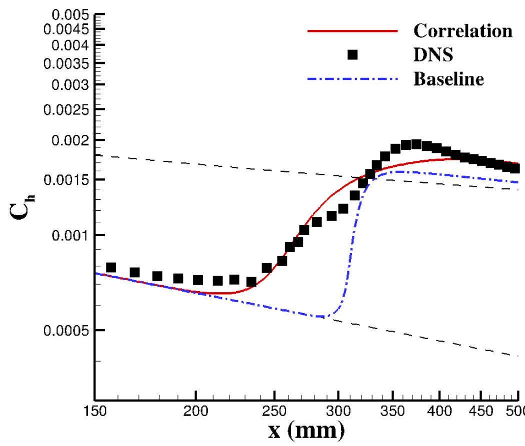


(d) M= 8.0, Re = 1.22×10$^7$

**Fig. 9 Transition predictions based on computations corresponding to the experiment of Grossir et al. [25] carried out in the VKI Longshot facility and the virtual tunnel DNS of transition over a 7-degree half angle cone at Mach 8 [30]. Intermittency is calculated using (a) the baseline intermittency model from previous coupled analysis [9] and (b) the correlation developed herein. The correlation is found to significantly improve the agreement with the experiment as compared to the baseline model.**

[8, 10]. This is not the case for hypersonics. As such, models for predicting the critical N-factor at transition and the intermittency characteristics of the transition zone are necessary for coupled CFD-stability analysis to be of practical use. Previous work by the authors demonstrated a correlation for the critical transition N-factor which produced good agreement with experimental data for canonical configurations studied in conventional hypersonic ground test facilities [15]. That correlation was designed to use input parameters that are often accessible using RANS CFD, including the facility disturbance level, the freestream flow parameters, and simple geometric inputs such as the leading-edge or nose radius. The present paper complements that work by presenting a correlation for the intermittency evolution.

A data-driven correlation to predict the intermittency distribution for use with coupled RANS-stability transition prediction has been developed. This new correlation relies on a modification to the implementation of the SA turbulence model in OVERFLOW to allow for larger freestream values of $\mu_T$ without negatively impacting the laminar boundary layer upstream of transition. This correlation is trained on a library of canonical ground and flight test cases selected from the available literature. The intermittency parameters in the training database are identified via a black-box algorithm which seeks to identify the intermittency parameters that minimize the relative error in surface heat transfer between the experimental data from selected test cases used for model training and the corresponding CFD simulations. Based on this training data, a correlation has been developed for canonical ground test cases along with a preliminary correlation for flight test data. The ground test correlation is shown to produce significant improvements in transition zone heat flux as compared to experiments for four additional ground test cases.

The primary correlation developed in this work, which is based on ground test facility data for supersonic and hypersonic canonical configurations, is based on the computational intermittency function

$$\gamma = (1 + C_{ov})(1 - exp(-\eta_1 \zeta_1^2)) - C_{ov}(1 - exp(-\eta_2 \zeta_2^2)), \tag{21}$$

whose constants are determined as correlations of the flow and transition parameters. The nondimensional transition zone width, necessary to calculate the coordinates $\zeta_1$ and $\zeta_2$ is calculated as

$$\Delta Re_1 = 4.20465 \times 10^{-26} \alpha_{t,1}^3 - 7.80382 \times 10^{-15} \alpha_{t,1}^2 + 3.18556 \times 10^{-4} \alpha_{t,1} + 1.75343 \times 10^5, \tag{22}$$

where

$$\alpha_{t,1} = Re_\infty M_\infty^{3.43} (T_w/T_{tot})^{0.42}. \tag{23}$$

The primary transition exponent $\eta_1$ is then calculated as

$$\eta_1 = 0.0034[(\Delta Re_1/Re_{onset})^{1/2} Re_\infty M_\infty^2 (T_w/T_{tot})]^{0.28198} \tag{24}$$

and the overshoot parameter is calculated as

$$C_{ov} = \max[\min[1.0, 3.047 \times 10^{-10}(Re_\infty M_\infty^3) - 0.5907], 1.0], \tag{25}$$

which is only considered for cases that satisfy

$$3.5 < M_\infty < 10.0. \tag{26}$$

For cases with nonzero values of $C_{ov}$,

$$\frac{\eta_2}{\eta_1} = \tanh[2.464 \times 10^{-7}(Re_\infty - 1545891)] + 1.02, \tag{27}$$

and

$$\Delta Re_2 = \Delta Re_1. \tag{28}$$

For cases where $C_{ov} \approx 0$, Eqs. 27 and 28 can be omitted, as these parameters have no influence on the distribution of $\gamma$.

This correlation, combined with the modification to the implementation of the SA turbulence model has been demonstrated to provide significant improvements to visual agreement with experimental heat transfer data in the transition region for high-speed ground test cases. This correlation also provides a basis to estimate the degree of transition overshoot which can be expected in hypersonic flows for which it is valid. Future work will seek to expand the set of flows for which the correlation is applicable, integrate additional information accessible in a coupled CFD-stability context to the correlation to improve its accuracy, and explore combining the existing ground and flight test correlations into a single relationship.

The next planned step in the advancement of the present work will be an examination of the influence of pressure gradient on transition zone characteristics for ground test facilities, utilizing the flared cone experiments of Kimmel et al. [29] as a basis for these insights. Future work will explore the possibility of improving the present correlation via the inclusion of the transition N-factor or other parameters, as well as potentially adding additional test cases to increase the confidence in the flight test correlation. The application of the present model to SST-based transition prediction will be explored, and a similar model specifically intended for use with SST may be developed. The low-Reynolds number cases will be supplemented so as to disambiguate the influence of Reynolds number and pressure gradient. Additionally, there is potential for additional data to increase the predictive capability of the present correlation, and cases with multi-mode transition (such as the BOLT) configuration could be considered in follow-on work.

## Acknowledgments

This research is sponsored by the NASA Hypersonic Technology Project (HTP) under the Aeronautics Research Mission Directorate. Computations included in this work were utilized the LaRC K Cluster along with the computational resources provided by the NASA High-End Computing (HEC) Program through the NASA Advanced Supercomputing (NAS) Division at the Ames Research Center. The authors also thank Prof. Lian Duan for sharing the virtual tunnel DNS data utilized in this work.

# References


[1] Anderson Jr, J. D., *Hypersonic and High-Temperature Gas Dynamics*, American Institute of Aeronautics and Astronautics, 2019. https://doi.org/10.2514/4.105142, 3rd Edition.

[2] Veerasamy, D., and Atkin, C., "A Rational Method for Determining Intermittency in the Transitional Boundary Layer," *Experiments in Fluids*, Vol. 61, No. 11, 2020. https://doi.org/10.1007/s00348-019-2856-5.

[3] Franko, K. J., and Lele, S. K., "Breakdown Mechanisms and Heat Transfer Overshoot in Hypersonic Zero Pressure Gradient Boundary Layers," *Journal of Fluid Mechanics*, Vol. 730, 2013, p. 491–532. https://doi.org/10.1017/jfm.2013.350.

[4] Horvath, T. J., Berry, S. A., Hollis, B. R., Chang, C.-L., and Singer, B. A., "Boundary Layer Transition on Slender Cones in Conventional and Low Disturbance Mach 6 Wind Tunnels," *AIAA Paper 2002-2743*, 2002. https://doi.org/10.2514/6.2002-2743.

[5] Qiao, L., Xu, J., Bai, J., and Zhang, Y., "Fully Local Transition Closure Model for Hypersonic Boundary Layers Considering Crossflow Effects," *AIAA Journal*, Vol. 59, No. 5, 2021. https://doi.org/10.2514/1.J059765.

[6] Liu, Z., Lu, Y., Li, J., and Yan, C., "Local Correlation-Based Transition Model for High-Speed Flows," *AIAA Journal*, Vol. 60, No. 3, 2022, pp. 1365–1381. https://doi.org/10.2514/1.J060994.

[7] Papp, J. L., and Dash, S. M., "Hypersonic Transitional Modeling for Scramjet and Missile Applications," *AIAA 2002-155*, 2002. https://doi.org/10.2514/6.2002-155.

[8] Venkatachari, B. S., Carnes, J. A., Chang, C.-L., and Choudhari, M., "Boundary-Layer Transition Prediction Through Loose Coupling of OVERFLOW and LASTRAC," *AIAA Paper 2022-3682*, 2022. https://doi.org/10.2514/6.2022-3682.

[9] Vogel, E. A., Venkatachari, B. S., Li, F., Paredes, P., and Choudhari, M., "CFD Integrated Transition Modeling for High-Speed Flows via Coupled OVERFLOW-LASTRAC Analysis," *AIAA Paper 2023-0438*, 2023. https://doi.org/10.2514/6.2023-0438.

[10] Hildebrand, N., Chang, C.-L., Choudhari, M. M., Li, F., Nielson, E., Venkatachari, B. S., and Paredes, P., "Coupling of the FUN3D Unstructured Flow Solver to the LASTRAC Stability Code to Model Transition," *AIAA Paper 2022-1952*, 2022. https://doi.org/10.2514/6.2022-1952.

[11] Narasimha, R., "The Laminar-Turbulent Transition Zone in the Boundary Layer," *Progress in Aerospace Sciences*, Vol. 22, 1985, pp. 29–80. https://doi.org/10.1016/0376-0421(85)90004-1.

[12] Spalart, P. R., and Allmaras, S. R., "A One-Equation Turbulence Model for Aerodynamic Flows," *AIAA Paper 1992-439*, 1994. https://doi.org/10.2514/6.1992-439.

[13] Nichols, R. H., and Buning, P. G., *User's Manual for OVERFLOW 2.3*, NASA Langley Research Center, Hampton, VA, August 2010.

[14] Chang, C.-L., "LASTRAC.3d: Transition Prediction in 3D Boundary Layers," *AIAA Paper 2004-2542*, 2004. https://doi.org/10.2514/62004-2542.

[15] Vogel, E., and Choudhari, M. M., "Enhancements to Linear Stability Solver-Based CFD-integrated Transition Prediction for High-Speed Flows," *AIAA Paper 2024-1159*, 2024. https://doi.org/10.2514/6.2024-1159.

[16] Vogel, E. A., Venkatachari, B. S., and Choudhari, M., "Verification of Two High-Speed Transition Models in OVERFLOW," 2023. In Preparation.

[17] Wagner, A., Kuhn, M., Schramm, J. M., and Hannemann, K., "Experiments on Passive Hypersonic Boundary layer control using ultrasonically absorptive carbon–carbon material with random microstructure," *Experiments in Fluids*, Vol. 54, No. 10, 2013, pp. 1606–1616. https://doi.org/10.1007/s00348-013-1606-3.

[18] MacLean, M., Mundy, E., Wadhams, T., Holden, M., Johnson, H., and Candler, G., "Comparisons of Transition Prediction Using PSE-Chem to Measurements for a Shock Tunnel Environment," *AIAA Paper 2007-4490*, 2007. https://doi.org/10.2514/6.2007-4490.

[19] Chen, F.-J., Malik, M. R., and Beckwith, I. E., "Boundary-Layer Transition on a Cone and Flat Plate at Mach 3.5," *AIAA Journal*, Vol. 27, No. 6, 1989. https://doi.org/10.2514/3.10166.

[20] Marineau, E. C., Moraru, G., Lewis, D. R., Norris, J. D., Lafferty, J. F., and Johnson, H. B., "Investigation of Mach 10 Boundary Layer Stability of Sharp Cones at Angle-of-Attack, Part 1: Experiments," *AIAA Paper 2015-1737*, 2015. https://doi.org/10.2514/6.2015-1737.

[21] Marineau, E. C., "Prediction Methodology for Second-Mode-Dominated Boundary-Layer Transition in Wind Tunnels," *AIAA Journal*, Vol. 55, No. 2, 2017, pp. 484–499. https://doi.org/10.2514/1.J05506.

[22] Boudreau, A. H., "Performance and Operational Characteristics of AEDC/VKF Tunnels A, B, and C," AEDC-TR-80-48, July 1981.

[23] Kimmel, R. L., Adamczak, D., Paull, A., Paull, R., Shannon, J., Pietsch, R., Frost, M., and Alesi, H., "HIFiRE-1 Ascent-Phase Boundary-Layer Tranition," *Journal of Spacecraft and Rockets*, Vol. 52, No. 1, 2015, pp. 217–230. https://doi.org/10.2514/1.A32851.

[24] Merlet, C. F., and Rumsey, C. B., "Supersonic Free-Flight Measurements of Heat Transfer and Transition on a 10 degree Cone having a Low Temperature Ratio," , March 1961. NASA TN D-951.

[25] Grossir, G., Masutti, D., and Chazot, O., "Flow characterization and boundary layer transition studies in VKI hypersonic facilities (Invited)," *AIAA Paper 2015-0578*, 2015. https://doi.org/10.2514/6.2015-0578.

[26] Park, S. H., Lee, J., and Kwon, J., "Preconditioned HLLE Method for Flows of all Mach numbers," *AIAA Journal*, Vol. 44, No. 11, 2006, pp. 2645 – 2653.

[27] Krishna, L. B., "On the Convergence of the Symmetric Successive Overrelaxation Method," *Linear Algebra and its Applications*, Vol. 56, No. 1, 1984, pp. 185 – 194.

[28] van Albada, G. D., van Leer, B., and Roberts Jr, W. W., "A Comparative Study of Computational Methods in Cosmic Gas Dynamics," *Astronomy and Astrophysics*, Vol. 108, No. 1, 1982, pp. 76 – 82.

[29] Kimmel, R., Poggie, J., and Schmisseur, J., *Effect of pressure gradients on axisymmetric hypersonic boundary layer stability*, 1993. https://doi.org/10.2514/6.2000-538.

[30] Schuabb, M., Duan, L., Casper, K., Wagnild, R., Choudhari, M. M., and Paredes, P., "Hypersonic Boundary-Layer Transition over a Circular Cone in Mach 8 Digital Wind Tunnel," , 2024. Submitted for Publication.

[31] Narasimha, R., "The laminar-turbulent transition zone in the boundary layer," *Progress in Aerospace Sciences*, Vol. 22, No. 1, 1985, pp. 29–80. https://doi.org/https://doi.org/10.1016/0376-0421(85)90004-1, URL https://www.sciencedirect.com/science/article/pii/0376042185900041.

[32] Raghunat, S., Mee, D., and Narashima, R., "Dependence of Turbulent Spot Initiation Rates on Hypersonic Boundary Layer Flow Parametersy," Vol. 55, No. 11, 2017, pp. 3640–3647. https://doi.org/https://doi.org/10.2514/1.J055502.

[33] Raghunat, S., Mee, D., and Narashima, R., *Dependence of Turbulent Spot Initiation Rates on Hypersonic Boundary Layer Flow Parametersy*, 2017. https://doi.org/10.2514/6.2017-1684.

[34] Johnson, H., Alba, C., Candler, G., MacLean, M., Wadhams, T., and Holden, M., "Boundary Layer Stability Analysis to Support the HIFiRE Transition Experiment," *AIAA Paper 2007-1159*, 2007. https://doi.org/10.2514/6.2007-311.

[35] Li, F., Choudhari, M., Chang, C.-L., Kimmel, R., Adamczak, D., and Smith, M., "Transition Analysis for the Ascent Phase of HIFiRE-1 Flight Experiment," *Journal of Spacecraft and Rockets*, Vol. 52, No. 2, 2015, pp. 1283–1293. https://doi.org/10.2514/1.A33258.